

Article

# Exclusive Particle Production in pp and pPb Collisions at CMS

Oliver Suranyi

MTA-ELTE Lendület CMS Particle and Nuclear Physics Group, Eötvös Loránd University, H-1117 Budapest, Hungary; oliver.suranyi@cern.ch

Received: 2 November 2017; Accepted: 2 December 2017; Published: 5 February 2018

**Abstract:** Exclusive processes provide a useful method to study a broad range of high energy physics fields from gluon density evolutions to searches for new physics. Three measurements from the Compact Muon Solenoid experiment are reviewed. Exclusive  $\pi\pi$  production is studied in proton–proton collisions. Low-mass meson resonances are observed in the invariant mass distribution of pion pairs. The total exclusive  $\pi^+\pi^-$  cross-section is also measured in the  $p_T(\pi) > 0.2$  GeV,  $|y| < 2$  region, yielding  $26.5 \pm 0.3$  (stat)  $\pm 5.0$  (syst)  $\pm 1.1$  (lumi)  $\mu\text{b}$ . The photoproduction of  $Y(nS)$  mesons is observed in ultraperipheral pPb collisions. The differential cross-sections are measured as a function of  $|t|$  and  $y$ . The comparison with previous measurements and theoretical models provides a better understanding of the gluon density evolution at low  $x$  values. Evidence for the  $\gamma\gamma \rightarrow W^+W^-$  process is shown with a  $3.7\sigma$  observed significance. According to the results, limits on anomalous quartic gauge couplings can be provided.

**Keywords:** exclusive physics; ultraperipheral collisions; anomalous couplings

## 1. Introduction

In high-energy physics, exclusive processes are a special type of collision where both colliding particles remain intact and we observe all of the produced particles. These can be either electroweak (two-photon fusion), strong (double pomeron exchange), or mixed electromagnetic and strong (photoproduction) processes. One of the greatest advantages of these collisions is that there are constraints on quantum numbers of the final state. This property is useful in a wide variety of high-energy research, such as searches for glueballs or the measurement of anomalous quartic gauge couplings. This paper introduces three results from Compact Muon Solenoid (CMS) experiment [1]: the study of exclusive and semi-exclusive  $\pi^+\pi^-$  production in proton–proton collisions at  $\sqrt{s} = 7$  TeV [2], the measurement of  $Y$  photoproduction in ultraperipheral pPb collisions [3] and the search for  $W$ -boson pairs produced via two-photon fusion in pp collisions and limits on anomalous quartic gauge couplings [4].

## 2. Exclusive and Semi-Exclusive $\pi^+\pi^-$ Production in Proton–Proton Collisions at $\sqrt{s} = 7$ TeV

Studying exclusive and semi-exclusive dipion production provides a good opportunity to study certain low mass resonances, since the quantum numbers of the final state are restricted by the exchanged objects. In these processes, two pions are produced centrally, while the two colliding protons remain intact (exclusive) or dissociate into the  $|\eta| > 4.9$  region (semi-exclusive), producing particles that cannot be detected by the forward calorimeter of the CMS detector. The two dominant processes are the double pomeron exchange (DPE) and the vector meson photoproduction (VMP)—the graphs of these processes are shown in Figure 1. Since pomerons have the quantum numbers of the vacuum, the final states in a DPE process can have  $J^{PC} = \{0^{++}, 2^{++}, 4^{++}, \dots\}$  and  $I^G = 0^+$  quantum numbers, where  $J$  is the total angular momentum,  $P$  is the parity,  $C$  is the charge parity,  $I$  is the isospin,

and  $G = C \cdot (-1)^I$ . Similarly, the final states allowed in VMP processes are restricted by the quantum numbers of the photon:  $J^{PC} = 1^{--}$  and  $I = \{0, 1\}$ . DPE processes provide a gluon-rich environment, which makes them suitable for glueball search.

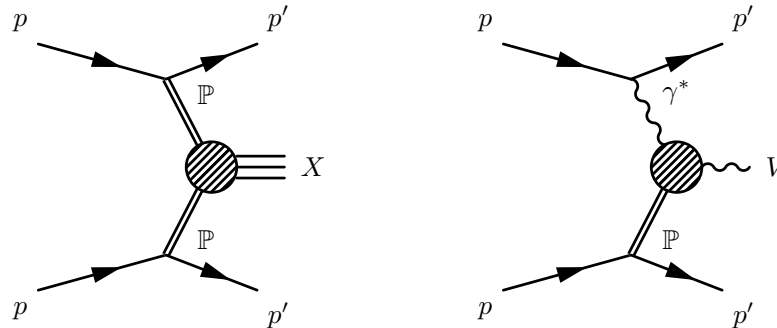


**Figure 1.** Graphs of (left) double pomeron exchange (DPE) and (right) vector meson photoproduction (VMP). The notation  $\gamma^*$  stands for a virtual photon and  $\mathbb{P}$  denotes pomeron.

Special low pileup data was collected at  $\sqrt{s} = 7$  TeV by the CMS detector in 2012, corresponding to  $450 \mu\text{b}^{-1}$  integrated luminosity. The data collection was triggered on bunch-crossings with no further requirement (zero bias). Several event selection criteria are applied on the zero bias events to select exclusive dihadron events. First, two good quality (in terms of  $\chi^2$ ) tracks with opposite sign are required. These should originate from the same interaction, and there should not be any other interactions in the event. Exclusivity is reached by rejecting events with activity in the calorimeters, except in a  $\Delta R < 0.1$  cone around track hits. The kinematic region of the analysis is  $p_T(\text{track}) > 0.2$  GeV and  $|y(\text{track})| < 2$ , where the rapidity is calculated assuming  $\pi^\pm$  mass. The final results are calculated as a function of following kinematic variables: invariant mass, transverse momentum, and rapidity, assuming  $\pi\pi$  pairs.

If an event fulfills all of the above criteria but contains one or more undetected particle, it contributes to the inclusive background. To estimate this contribution, a sample is used where all of the above selections are performed, except the calorimeter criteria. The distribution of events as a function of extra calorimeter hits is shown in Figure 2. This distribution is fitted with a negative binomial distribution, which is commonly used to fit multiplicity distributions. Events from the side-band region with 2–10 extra calorimeter hits are used to construct a background template as a function of kinematic variables listed above. The normalization of the background is calculated from the negative binomial fit.

The differential cross-sections shown in Figure 3 are unfolded by an iterative Bayesian method using early stopping as a regularization. The results are compared with the Minimum Bias Rockefeller (MBR) model of Pythia 8, Dime MC and STARlight Monte Carlo (MC) event generators. The MBR model describes DPE with a renormalized pomeron flux model. The Dime MC is capable to model continuum  $\pi^+\pi^-$  production in DPE—this is when the dipion pair is produced directly without any intermediate resonance, resulting in a smooth mass spectrum. The STARlight generator is used to generate  $\rho^0 \rightarrow \pi^+\pi^-$  VMP events. None of these simulations describe the low mass scalar and tensor resonances  $f_0(500)$ ,  $f_0(980)$ , and  $f_2(1270)$ . A slightly larger cross-section is measured in the mass region of  $\rho(770)$ , since the forward proton dissociation of semi-exclusive processes is not modelled by the MC event generators. There is a sharp drop at around 1 GeV in the mass spectrum, which was seen by several previous experiments [5] and can be interpreted as the interference of the  $f_0(980)$  resonance with the continuum production channel. There is a significant peak at 1.2–1.3 GeV, which is consistent with the parameters of the  $f_2(1270)$  resonance. The total cross-section calculated in the kinematic region  $p_T(\pi) > 0.2$  GeV and  $|y(\pi)| < 2$  is:

$$\sigma(pp \rightarrow p^* + \pi^+ \pi^- + p^*) = 26.5 \pm 0.3 (\text{stat}) \pm 5.0 (\text{syst}) \pm 1.1 (\text{lumi}) \mu\text{b}. \quad (1)$$

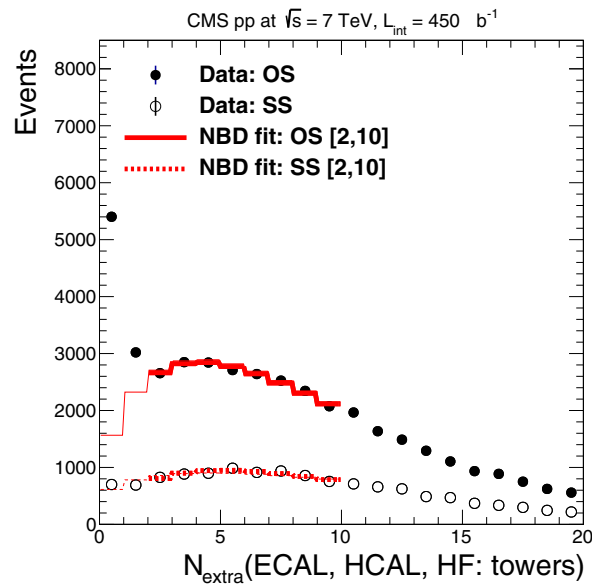


**Figure 2.** The distribution of events as a function of extra calorimeter hits in with opposite sign (OS) and same sign (SS) track pairs. A background template is constructed from the region from 2–10 extra calorimeter hits, and the normalization of the background is calculated from a negative binomial (NBD) fit. [2].

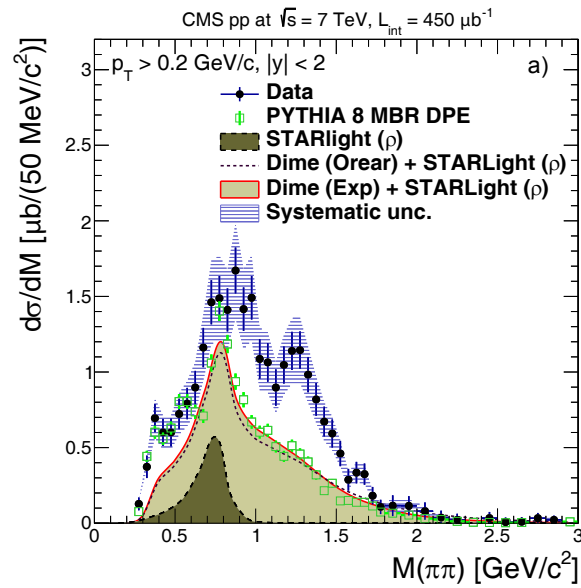


**Figure 3.** Cont.

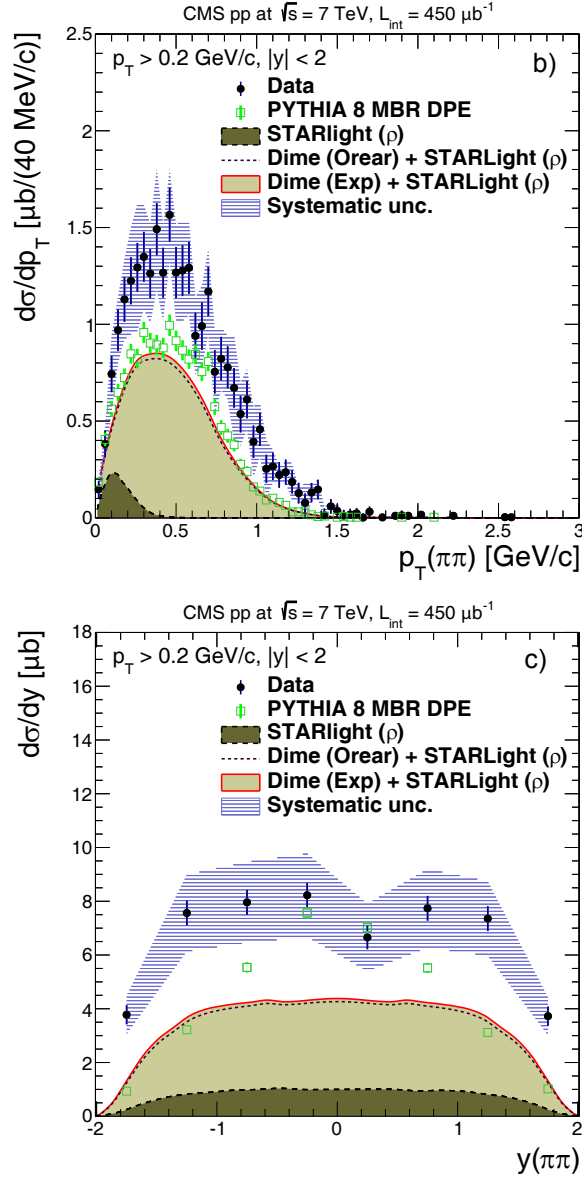


**Figure 3.** Differential cross section as a function of invariant mass (a), transverse momentum (b) and rapidity of the track pair (c), where all of the quantities are calculated with assuming  $\pi^+\pi^-$  masses [2]. The results are compared with the Minimum Bias Rockefeller (MBR) model of Pythia 8, Dime MC and STARlight Monte Carlo (MC) event generators.

### 3. Upsilon Photoproduction in Ultraperipheral pPb Collisions

In pPb collisions there is an enhanced photoproduction cross-section due to the high photon flux, which is proportional to  $Z^2$ . The production of  $Y(nS)$  can be described in a perturbative quantum chromodynamics (pQCD) and in a Regge theory framework—the corresponding graphs are shown in Figure 4. The cross-section of ultraperipheral  $Y(nS)$  production is related to the  $G(x, Q^2)$  gluon parton distribution function (PDF) of the proton:

$$\frac{d\sigma}{dt} \propto (x G(x, Q^2))^2, \quad (2)$$

therefore providing a method to probe the gluon density in the  $x \approx 10^{-2}$ – $10^{-4}$  region.

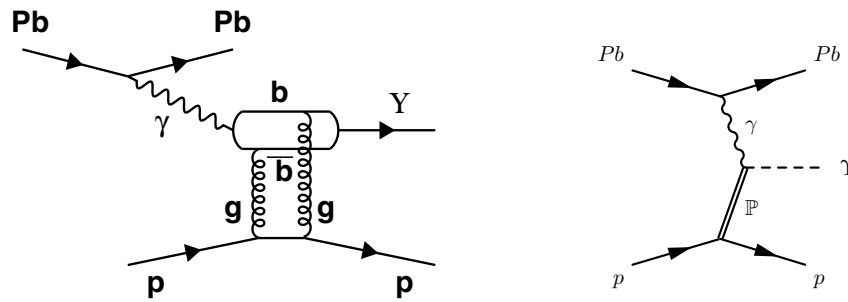


**Figure 4.** The graphs of  $p + Pb \rightarrow p + Y(ns) + Pb$  process (left) in the perturbative QCD and (right) in the Regge theory framework.

The data collected with the CMS experiment in 2013 was triggered on a single muon and 6 or less tracks in the tracker. The integrated luminosity of the dataset used in the measurement is  $32.6 \text{ nb}^{-1}$ . Further event selection criteria were applied at the offline level: the kinematic variables of muons are constrained as  $p_T(\mu) > 3.3 \text{ GeV}$  and  $|y(\mu)| < 2.2$ . Additionally,  $1 \text{ GeV}$  condition is required for the muon pair  $p_T(\mu\mu) \in [0.1, 1]$ . The low- $p_T(\mu\mu)$  cut is applied to reduce  $\gamma\gamma \rightarrow \mu\mu$  background, while the rejection of high- $p_T(\mu\mu)$  reduces the contribution from inclusive and semi-exclusive  $Y(ns)$  production. The invariant mass distribution of the  $\mu$  pairs is shown in Figure 5. The differential cross-sections shown in Figure 6 are calculated from the mass region from  $9.12\text{--}10.64 \text{ GeV}$  as a function of  $p_T^2(\mu\mu)$  and  $y(\mu\mu)$ .

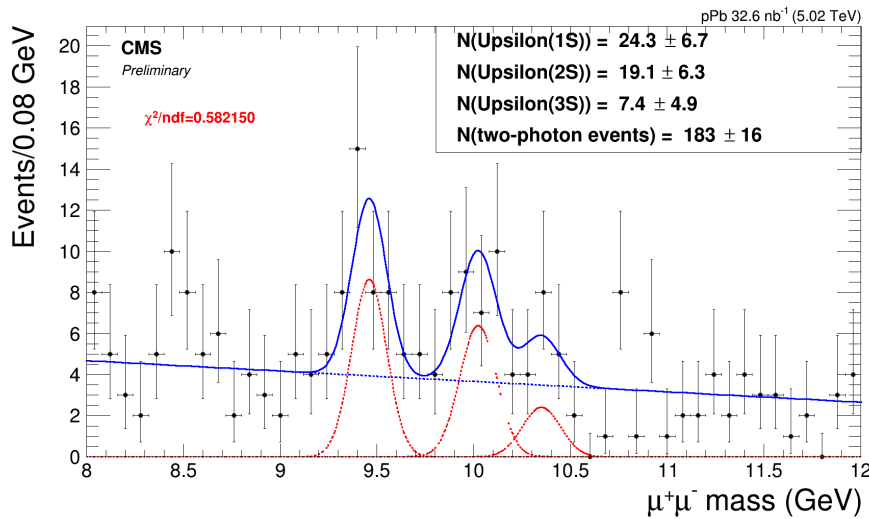


**Figure 5.** The invariant mass distribution of  $\mu$  pairs. The dashed red curves denotes the peaks corresponding to  $Y(ns)$ , the dashed blue line denotes the linear background, while the continuous blue curve stands for the sum of background and signal peaks.

There are five sources of background: quantum electrodynamics (QED) continuum production ( $\gamma\gamma \rightarrow \mu^+\mu^-$ ), inclusive  $Y$  production, Drell–Yan processes, semi-exclusive production, and  $\gamma Pb$  events (where the pomeron is emitted from the  $Pb$  nucleus and the photon is originating from the proton). The QED contribution is estimated by STARlight MC event generator, and it is normalized to the luminosity of the data. The inclusive  $Y$ , Drell–Yan, and semi-exclusive background is determined by a data-driven method, using a template created by loosening the event selection criteria, allowing at least one additional track with  $p_T > 2 \text{ GeV}$ . The normalization is calculated by comparing the template to signal sample in the  $p_T(\mu\mu) > 1.5 \text{ GeV}$  region, which is dominated by semi-exclusive and inclusive events.

The exclusive  $Y(nS)$  production is modelled by the STARlight event generator. For better description of the data, the generated events are reweighted to the observed cross-sections as

$$\frac{d\sigma}{d|t|} \propto e^{-b|t|}, \quad (3)$$

$$\sigma(W_{\gamma p}) \propto (W_{\gamma p})^\delta, \quad (4)$$

where  $t$  is the transferred momentum squared,  $W_{\gamma p} = 2E_p M_Y \exp(\pm y)$  is the photon proton center-of-mass energy, and  $b$  and  $\delta$  are fit parameters. Then,  $E_p$  is the energy of the proton,  $M_Y$  and  $y$  are mass and rapidity of the  $Y$  meson, respectively, and the  $\pm$  sign is defined according to the beam configuration ( $pPb$  or  $Pbp$ ). The result of reweighting is shown in Figure 6.

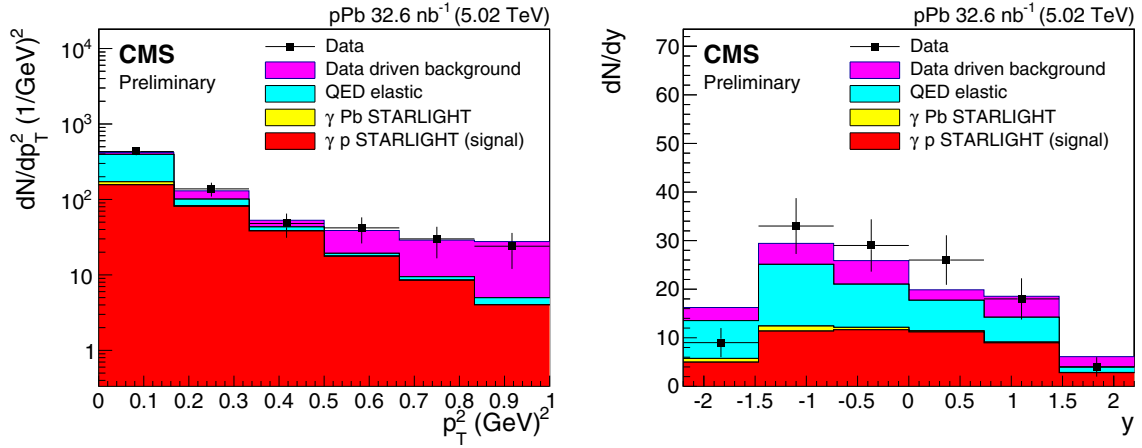


**Figure 6.** Differential cross-sections as a function of (left)  $p_T^2(\mu\mu)$  and (right)  $y(\mu\mu)$ , calculated from  $9.12 \text{ GeV} < M(\mu\mu) < 10.64 \text{ GeV}$  region. The results are compared with predictions from the STARlight event generator and data-driven background estimates [3]. QED stands for quantum electrodynamics.

The cross-sections as a function of  $|t|$  and  $W_{\gamma p}$  are shown in Figure 7, where  $p_T^2(\mu\mu) \approx |t|$  approximation is used to get  $d\sigma/d|t|$  and  $W_{\gamma p}$  is calculated from  $d\sigma/dy$  as

$$\sigma_{\gamma p} = \frac{1}{\phi} \frac{d\sigma_{Y(1S)}}{dy} \propto (W_{\gamma p})^2, \quad (5)$$

where  $\phi$  is photon flux, obtained from STARlight. An iterative Bayesian algorithm is used with an early stopping as regularization to correct for detector effects and data migration. An exponential fit is performed on  $d\sigma/d|t|$ :

$$\frac{d\sigma}{d|t|} = N e^{-b|t|}, \quad (6)$$

where  $N$  and  $b$  are the fit parameters. The obtained value of  $b$  is  $4.5 \pm 1.7$  (stat)  $\pm 0.6$  (syst)  $\text{GeV}^{-2}$ , which is compatible with HERA (Hadron-Electron Ring Accelerator) measurements (H1:  $4.73 \pm 0.25$  (stat)  $\text{GeV}^{-2}$  [6], Zeus:  $4.3_{-1.3}^{+2.0}$  (stat)  $\text{GeV}^{-2}$  [7]).

Since  $\sigma(W_{\gamma p})$  is related to the square of the gluon PDF, which can be well described with a power law behaviour at this regime of  $x$ , the  $\sigma(W_{\gamma p})$  is fitted with a power function  $A \times (W/400)^\delta$ , where  $A$  and  $\delta$  are fit parameters. The fit is performed for CMS only ( $\delta = 0.96 \pm 0.43$ ) and CMS+HERA ( $\delta = 0.94 \pm 0.28$ ) data points. The result disfavours the leading order Jones-Martin-Ryskin-Teubner (JMRT) model results, but it is consistent with the next-to-leading order JMRT prediction [8]. The fit is also compared to the factorized IPsat model [9], which is based on the color glass condensate (CGC) formalism, and the Iancu-Itakura-Munier (IIM) color dipole model [10]. These two predictions bracket the measured CMS+HERA data. Finally the impact-parameter color glass

condensate (bCGC) models [11], using meson wave functions to describe the  $t$ -dependence of differential cross-sections, are also compared to the results. The bCGC predictions systematically underestimate the cross-section, but are still consistent within uncertainties and correctly describe the rise of the cross-section.

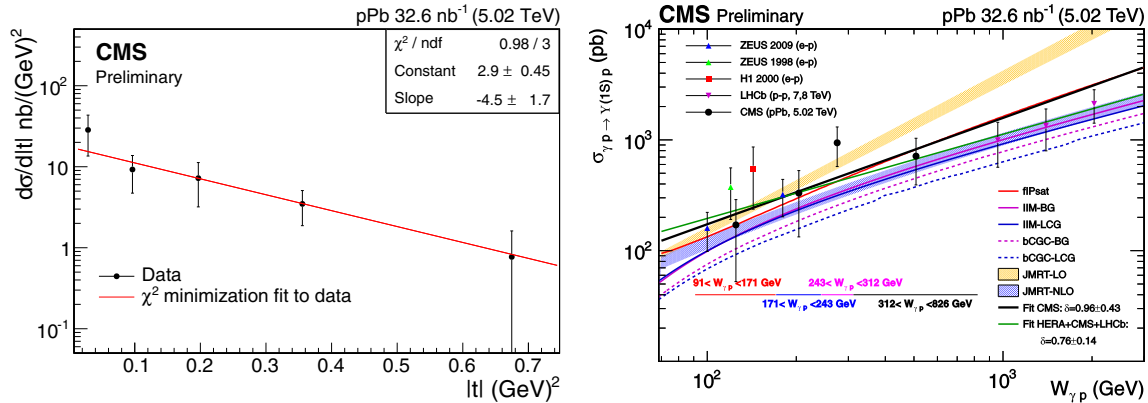


**Figure 7.** Cross-sections as a function of (left)  $|t|$  and (right)  $W_{\gamma p}$  [3]. The results are compared to measurements from LHCb (Large Hadron Collider beauty) experiment and HERA (Hadron-Electron Ring Accelerator) experiments ZEUS and H1. Predictions from various theoretical calculations are also shown here: IPsat model, IIM (Iancu-Itakura-Munier) color dipole formalism with two sets of meson wave functions: Boosted Gaussian (BG) and Light Cone Gaussian (LCG), impact-parameter color glass condensate (bCGC) models, LO (leading order) and NLO (next-to-leading order) JMRT (Jones-Martin-Ryskin-Teubner) models.

#### 4. Search for W-Boson Pairs Produced via Two-Photon Fusion in pp Collisions and Limits on Anomalous Quartic Gauge Couplings

The measurement of exclusive W-boson pair production provides information about electroweak gauge couplings. Any significant deviation from the Standard Model predictions can be a sign of new physics, like supersymmetry, extra dimensions, or additional gauge bosons. The leading order processes are shown in Figure 8—the contribution of the graph with the quartic coupling ( $\propto g^2 e^2$ , where  $g$  is the coupling constant of the weak interaction and  $e$  is the electron charge) is suppressed compared to the ones with triple coupling ( $\propto g e^2$ ).

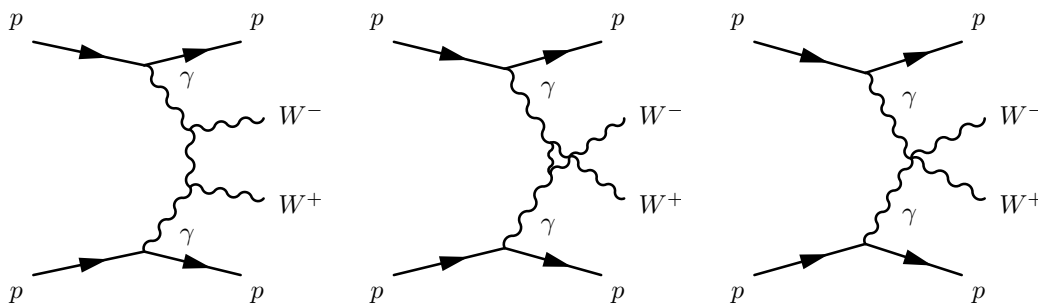


**Figure 8.** Leading order processes of exclusive  $W^+W^-$  production via two-photon fusion. The contribution of the third graph is suppressed compared to the other two due to the quartic gauge coupling.

The measurement is performed on both a 7 and 8 TeV dataset, corresponding to  $5.5 \text{ fb}^{-1}$  and  $19.7 \text{ fb}^{-1}$  integrated luminosity, respectively. The data collection is triggered on two leptons with

$p_T(\ell) > 17$  GeV for the leading and  $p_T(\ell) > 8$  GeV for the subleading lepton. The  $W$ -bosons are observed via their weak decay to lepton–antineutrino and antilepton–neutrino pairs:

$$pp \longrightarrow p^* + WW + p^* \longrightarrow p^* + \ell^+ \ell'^- \nu \bar{\nu} + p^*.$$

Therefore, selected events are required to have opposite sign, different flavour lepton pairs ( $e^\pm \mu^\mp$ ), originating from a common vertex with no other tracks. Further requirements are  $p_T(\mu)$ ,  $E_T(e) > 20$  GeV,  $|\eta(\mu, e)| < 2.4$ , and  $M(e\mu) > 20$  GeV. Another sample containing same-flavour lepton pairs is used as control sample. The signal region of the measurement is  $p_T(e\mu) > 30$  GeV. One or both protons can dissociate in the non-instrumented forward direction (semi-exclusive or elastic process). This contribution is accounted for by a correction factor calculated by a Monte Carlo-based method using high statistics channels ( $\gamma\gamma \rightarrow e^+e^-$  and  $\gamma\gamma \rightarrow \mu^+\mu^-$ ). There are four sources of background: inclusive diboson production,  $W$ +jets, Drell–Yan  $\tau^+\tau^-$  production, and  $\gamma\gamma \rightarrow \tau^+\tau^-$ , treated by various data-driven methods.

The measured distribution as a function of  $p_T(e\mu)$  is shown in Figure 9. The observed cross-section for process  $pp \rightarrow p^*(\gamma\gamma \rightarrow W^+W^- \rightarrow e^\pm \mu^\mp \nu \bar{\nu})p^*$  is  $2.2^{+3.3}_{-2.0}$  fb and  $11.9^{+5.6}_{-4.5}$  fb at 7 and 8 TeV, respectively. The Standard Model prediction at 7 TeV is  $4.0 \pm 0.7$  fb and  $6.9 \pm 0.6$  fb at 8 TeV, thus the measurements are consistent within uncertainties. The combined significance of the 7 and 8 TeV measurement is  $3.4 \sigma$ .

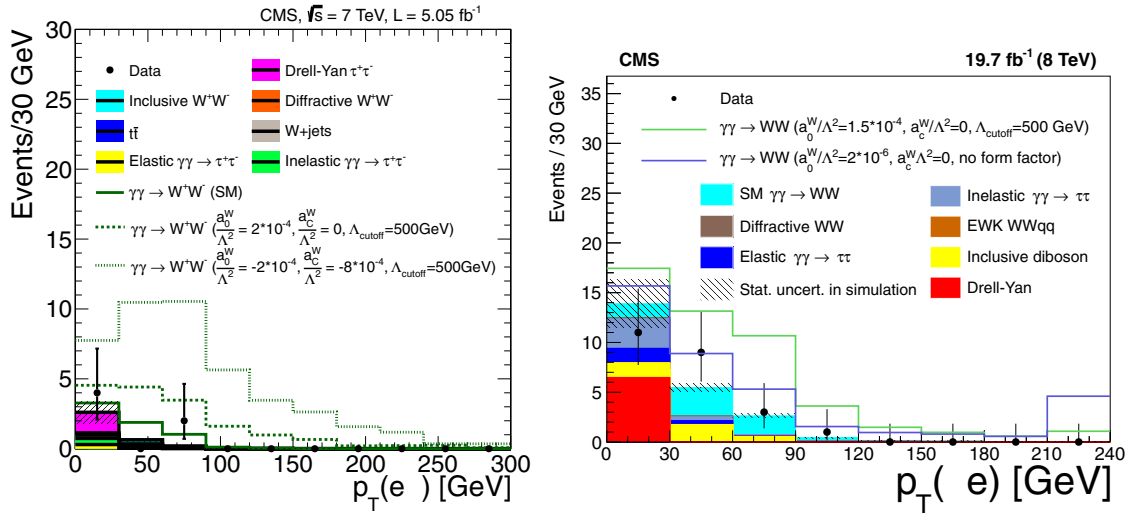
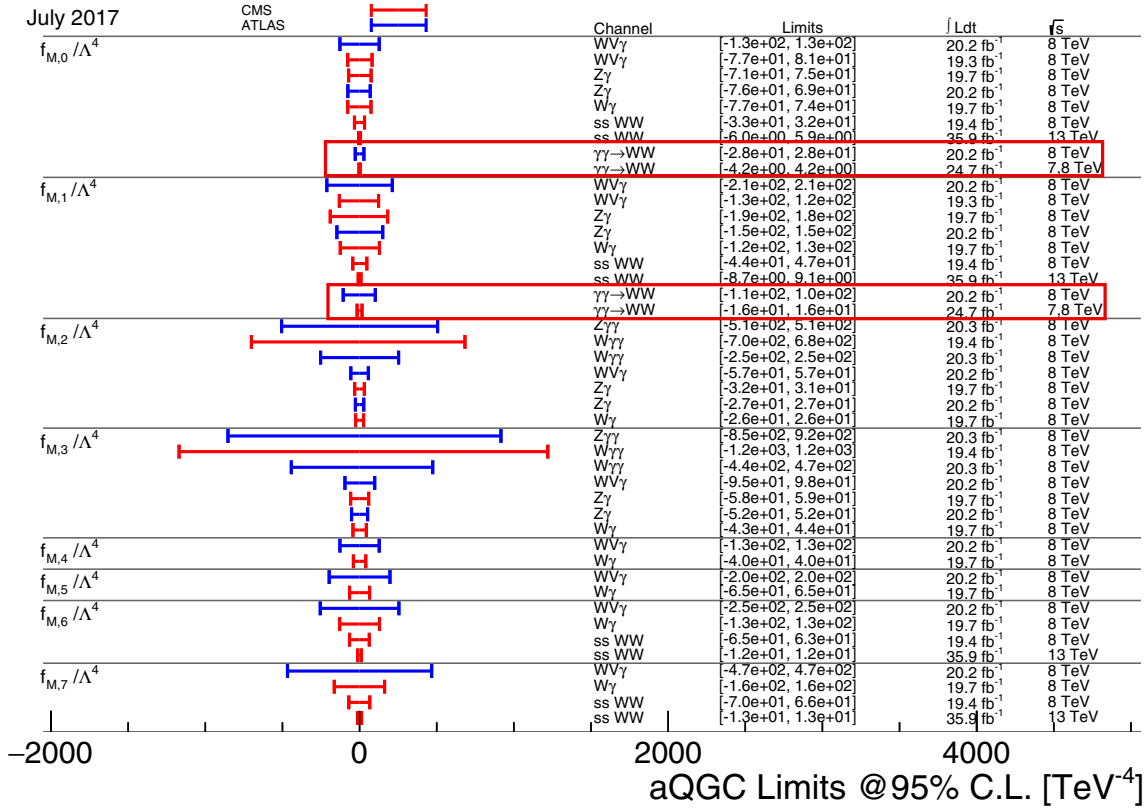


**Figure 9.**  $p_T(e\mu)$  distribution of exclusive  $W^+W^-$  events at (left) 7 TeV and (right) 8 TeV [4]. EWK stands for electroweak production channels.

The Standard Model only allows gauge couplings obeying gauge invariance. Effective models can have other gauge couplings, which would be the signs of new physics. These can be considered in the Lagrangian by adding extra terms; the simplest possible extension is the six-dimensional “LEP-legacy” model (LEP: Large Electron-Positron Collider),  $a_{0,C}^W$  and  $a_0^W$  are the so-called six-dimensional operators [12]. The next possible extension introduces the eight-dimensional operators ( $f_{M,0-3}$ ), which can be expressed with the six-dimensional ones [13,14]. The six-dimensional operators were ruled out by LEP, but they could be still used to calculate eight-dimensional operators by assuming a unitarity restoring form factor with  $\Lambda_{\text{cutoff}} = 500$  GeV:

$$a_{0,C}^W \longrightarrow \frac{a_{0,C}^W}{1 + \frac{W_{\gamma\gamma}}{\Lambda_{\text{cutoff}}}} \quad (7)$$

Combining the 7 and 8 TeV results, the following one-dimensional limits are obtained at 95% confidence level: the value of  $a_0^W/\Lambda^2$  is constrained in the range  $[-0.9, 0.9] \times 10^{-4} \text{ GeV}^{-2}$ , while  $a_C^W/\Lambda^2$  is within  $[-3.6, 3.0] \times 10^{-4} \text{ GeV}^{-2}$ . According to Figure 10 [15], this result gives the most stringent limit on  $f_{0,M}$  operator so far.



### 5. Conclusions

Exclusive processes are a versatile tool of high-energy physics. They are useful in a wide range of topics such as studying low mass meson resonances, evolution of gluon PDF at low  $x$  values, and testing Standard Model couplings to search for new physics. The differential cross-sections of  $\pi^+\pi^-$  final state is measured as a function of invariant mass, transverse momentum, and rapidity. A resonant structure is observed in the mass spectrum, which is a signature of low mass resonances. The observed features of these resonances are consistent with the  $\rho(770)$ ,  $f_0(980)$ , and  $f_2(1270)$  resonances. The evolution of gluon density function is studied at low  $x$  values via the production of  $\Upsilon(nS)$  states observed in pPb collisions. The results are consistent with previous HERA measurements, NLO JMRT model, color glass condensate, and color dipole models. The anomalous coupling  $WW\gamma\gamma$  couplings are studied via exclusive  $W^+W^-$  production. The measurement provides the most stringent limit on the  $f_{0,M}$  operator so far.

**Acknowledgments:** This work was supported by the ÚNKP-17-3 New National Excellence Program of the Ministry of Human Capacities, Hungarian Scientific Research Fund (K 109703), National Research, Development and Innovation Office of Hungary (K 124845, FK 123842) and Hungarian Academy of Sciences "Lendület" (Momentum) Program (LP 2015-7/2015).

**Conflicts of Interest:** The author declare no conflict of interest.

## References

1. CMS Collaboration. The CMS experiment at the CERN LHC. *JINST* **2008**, *3*, S08004.
2. CMS Collaboration. Exclusive and semi-exclusive  $\pi^+\pi^-$  production in proton-proton collisions at  $\sqrt{s} = 7$  TeV. *arXiv* **2017**, arXiv:hep-ex/1706.08310.
3. CMS Collaboration. Measurement of exclusive Y photoproduction in pPb collisions at  $\sqrt{s_{NN}} = 5.02$  TeV. Available online: <http://cds.cern.ch/record/2147428> (accessed on 26 December 2017).
4. CMS Collaboration. Evidence for exclusive  $\gamma\gamma \rightarrow W^+W^-$  production and constraints on anomalous quartic gauge couplings in  $pp$  collisions at  $\sqrt{s} = 7$  and 8 TeV. *J. High Energy Phys.* **2016**, *8*, 119.
5. Barberis, D.; Beusch, W.; Binon, F.G.; Blick, A.M.; Close, F.E.; Danielsen, K.M.; Dolgoplov, A.V.; Donskov, S.V.; Earl, B.C.; Evans, D.; et al. A Partial wave analysis of the centrally produced  $\pi^+\pi^-$  system in  $pp$  interactions at 450 GeV/c. *Phys. Lett. B* **1999**, *453*, 316–324.
6. Adloff, C.; Andreev, V.; Andrieu, B.; Arkadov, V.; Astvatsatourov, A.; Ayyaz, I.; Babaev, A.; Bähr, J.; Baranov, P.; Barrelet, E.; et al. Elastic photoproduction of  $J/\psi$  and Y mesons at HERA. *Phys. Lett. B* **2000**, *483*, 23–35.
7. Abramowicz, H.; Abt, I.; Adamczyk, L.; Adamus, M.; Aggarwal, R.; Antonelli, S.; Antonioli, P.; Antonov, A.; Arneodo, M.; Aushev, V.; et al. Measurement of the t dependence in exclusive photoproduction of Y(1S) mesons at HERA. *Phys. Lett. B* **2012**, *708*, 14–20.
8. Jones, S.P.; Martin, A.D.; Ryskin, M.G.; Teubner, T. Probes of the small x gluon via exclusive  $J/\psi$  and Y production at HERA and the LHC. *J. High Energy Phys.* **2013**, *11*, 085.
9. Lappi, T.; Mantysaari, H.  $J/\psi$  production in ultraperipheral Pb+Pb and p+Pb collisions at energies available at the CERN Large Hadron Collider. *Phys. Rev. C* **2013**, *87*, 032201.
10. Sampaio dos Santos, G.; Machado, M.V.T. On theoretical uncertainty of color dipole phenomenology in the  $J/\psi$  and Y photoproduction in pA and AA collisions at the CERN Large Hadron Collider. *J. Phys. G* **2015**, *42*, 105001.
11. Gonçalves, V.P.; Moreira, B.D.; Navarra, F.S. Exclusive Y photoproduction in hadronic collisions at CERN LHC energies. *Phys. Lett. B* **2015**, *742*, 172–177.
12. Belanger, G.; Boudjema, F. Probing quartic couplings of weak bosons through three vectors production at a 500-GeV NLC. *Phys. Lett. B* **1992**, *288*, 201–209.
13. CMS Collaboration. Search for  $WW\gamma$  and  $WZ\gamma$  production and constraints on anomalous quartic gauge couplings in  $pp$  collisions at  $\sqrt{s} = 8$  TeV. *Phys. Rev. D* **2014**, *90*, 032008.
14. Belanger, G.; Boudjema, F.; Kurihara, Y.; Perret-Gallix, D.; Semenov, A. Bosonic quartic couplings at LEP-2. *Eur. Phys. J. C* **2000**, *13*, 283–293.
15. Limits on Anomalous Triple and Quartic Gauge Couplings. Available online: <https://twiki.cern.ch/twiki/bin/view/CMSPublic/PhysicsResultsSMPaTGC> (accessed on 26 December 2017).

